Proceedings of the 12th International Conference on the Stability of Ships and Ocean Vehicles, 14-19 June 2015, Glasgow, UK.

Non-stationary Ship Motion Analysis Using Discrete Wavelet Transform

Toshio, ISEKI, *Tokyo University of Marine Science and Technology* iseki@kaiyodai.ac.jp

ABSTRACT

The discrete wavelet transform is applied to non-stationary ship motion data. The data was obtained by on-board measurements that were carried out under relatively severe sea conditions. In the full scale measurements, the ship travelled on several courses to investigate the change of frequency response relative to the encounter wave angle. Comparing to the results of Fourier analysis and time-varying autoregressive coefficient modelling, it is shown that the discrete wavelet transform can analyse non-stationary ship motions in the frequency and the time domain.

Keywords: *seakeeping, discrete wavelet transform, full-scale ship measurements, non-stationary time series*

1. INTRODUCTION

The author has been trying to develop a guidance system for heavy weather operation and investigating suitable signal processing methods under the necessity of analysing non-stationary stochastic process. Generally, the assumption of stationary stochastic processes is applied to the seaway, but not to ship response because it also depends on ship manoeuvres. Ship response is strongly affected by changes in the encounter angle and frequency of waves. Therefore, the method is needed to be a real-time algorithm that can deal with non-stationary stochastic processes. In the previous study (Iseki & Terada, 2002, Iseki, 2006), the instantaneous spectral analysis with the Time-Varying coefficient Vector Auto Regressive (TVVAR) model was introduced to deal with non-stationary ship motions. Some problems, however, were pointed out because the maximum likelihood method for determination of the trade-off parameter, which is the ratio of the observation noise and the system noise of Kalman filter, cannot be applied to the real-time algorithm.

On the other hand, the Discrete Wavelet Transform (DWT) is widely used recently in the field of signal processing (Percival and Walden 2000), image compression and analyses of non-stationary time series. In comparison with the Continuous Wavelet Trans-form (CWT), the process of DWT can be recognized as decomposition of a time series with use of digital filters while the CWT is defined by a convolution integral over entire time axis. In this sense, the DWT is suitable for digital computing and real-time analyses of non-stationary time series.

The author was also applied the Discrete Wavelet Packet Transform (DWPT) to non-stationary ship motion data (Kang and Iseki 2013). Comparing to the results of Discrete Fourier Transform (DFT) and the TVVAR modelling, it was confirmed that the locations of peaks of the DWPT coefficients agree well with the peak frequencies of the spectra estimated by DFT. However, the obvious advantage of DWPT was not observed in comparison with TVVAR modelling.

In this paper, both of DWT and DWPT are applied to analyses of non-stationary ship motion data which was measured during a large course alteration. Comparing to the results of DFT and TVVAR modelling, the validity of the DWT and DWPT is discussed in detail.

2. DISCRETE WAVELET TRANSFORM

2.1 Basic Properties

The DWT of a measured time series $\mathbf{X}=\{x_n : n=0,1,2,\cdots,N-1\}$ is defined as follows:

$$\mathbf{W}=\mathbf{wX} \tag{1}$$

where $\mathbf{W}$ denotes an N dimensional column vector of DWT coefficients, $\mathbf{w}$ an $N\times N$ real-valued matrix defining the DWT.

For the convenience, we assume that the sample size $N=2^{J_0}$ for an integer J_0. The DWT coefficient $\mathbf{W}$ and matrix $\mathbf{w}$ could be separated as;

$$\mathbf{W}=\left[\mathbf{W}_1,\mathbf{W}_2,\cdots,\mathbf{W}_{J_0},\mathbf{V}_{J_0}\right]^T \tag{2}$$

$$\mathbf{w}=\left[\mathbf{w}_1,\mathbf{w}_2,\cdots,\mathbf{w}_{J_0},\mathbf{v}_{J_0}\right]^T \tag{3}$$

where

$$\mathbf{W}_j=\mathbf{w}_j\mathbf{X}^T,\quad \mathbf{V}_{J_0}=\mathbf{v}_{J_0}\mathbf{X}^T \tag{4}$$

The $\mathbf{W}_j$ and $\mathbf{V}_j$ are the wavelet coefficient sub-vector and the scaling coefficient sub-vector for the level j.

$$\mathbf{W}_j=\left[W_{j,1},W_{j,2},\cdots,W_{j,N_j}\right]^T \tag{5}$$

$$\mathbf{V}_j=\left[V_{j,1},V_{j,2},\cdots,V_{j,N_j}\right]^T \tag{6}$$

where $N_j\equiv N/2^j$ denotes the number of components at the level j. Therefore, $\mathbf{V}_{J_0}$ contains only a scaling coefficient.

The "level j" is closely related to the scale $\tau_j\equiv 2^{j-1}$ $(j=1,2,\cdots,J_0)$ which is the sampling interval of the time series and denotes the number of times of "down-sampling by two". If the actual sampling time is denoted by Δt (sec), the physical scale can be expressed by $\tau_j\Delta t$.

By orthonormality of the DWT, we can synthesize the vector $\mathbf{X}$ from $\mathbf{W}$ by,

$$\begin{aligned}\mathbf{X}=\mathbf{w}^T\mathbf{W}&=\sum_{j=1}^{J_0}\mathbf{w}_j^T\mathbf{W}_j+\mathbf{v}_{J_0}^T\mathbf{V}_{J_0}\\&=\sum_{j=1}^{J_0}\mathbf{D}_j+\mathbf{S}_{J_0}\end{aligned} \tag{7}$$

which is also a definition of Muti-Resolution Analysis (MRA) of $\mathbf{X}$. Here $\mathbf{D}_j$ and $\mathbf{S}_{J_0}$ are called as "details" for level j and "smooth" for level J_0, respectively. In the actual calculations, the DWT matrix $\mathbf{w}$ is not formed explicitly but rather $\mathbf{W}$ is computed using the "pyramid algorithm" which is effective and fast from the viewpoint of the computational process (Mallat 1989).

If we represent the actual wavelet filter by $\{h_l : l=0,1,2,\cdots,L-1\}$, we can also derive the scaling filter by using "quadrature mirror" relationship,

$$g_l\equiv(-1)^{l+1}h_{L-1-l} \tag{8}$$

where L denotes the width of the wavelet filter.

In practice, the wavelet filter $\{h_l\}$ is a high-pass filter, while the scaling filter $\{g_l\}$ is a low-pass filter. Assuming $\mathbf{V}_0=\mathbf{X}$ with defined $\{h_l\}$, $\{g_l\}$, general jth stage of the pyramid

algorithm yields the nth components of the sub-vector $\mathbf{W}_j$ and $\mathbf{V}_j$ as follows;

$$W_{j,n} \equiv \sum_{l=0}^{L-1} h_l V_{j-1,2n+1-l} \tag{9}$$

$$V_{j,n} \equiv \sum_{l=0}^{L-1} g_l V_{j-1,2n+1-l} \quad (n = 0, 1, 2, \cdots, N_j - 1) \tag{10}$$

Therefore, the DWT can be recognized as a decomposition of a time series $\mathbf{X}$ into coefficients that can be associated with different scales and times.

2.2 DWT spectrum

According to the decomposition described in the previous section, the power spectrum of DWT can be defined as follows;

$$P_W(\tau_j) \equiv \frac{1}{N}\left\|\mathbf{W}_j\right\|^2 \tag{11}$$

$$\sum_{j=1}^{J} P_W(\tau_j) = \frac{1}{N}\left\|\mathbf{W}_j\right\|^2 = \frac{1}{N}\left\|\mathbf{X}\right\|^2 - \overline{\mathbf{X}} = \sigma_{\mathbf{X}}^2 \tag{12}$$

where $\sigma_{\mathbf{X}}^2$ denotes the sample variance.

2.3 Wavelet Filters

The filter $\{h_{j,l}\}$ and $\{g_{j,l}\}$ are the band pass filters with pass band given by $1/\Delta t 2^{j+1} \le f \le 1/\Delta t 2^{j}$ and $0 \le f \le 1/\Delta t 2^{j+1}$ (Hz), respectively. Meanwhile, scaling filters as well as wavelet filters must satisfy the three basic properties, which are

$$\sum_{l=0}^{L-1} g_l = \sqrt{2}, \quad \sum_{l=0}^{L-1} g_l^2 = 1 \tag{13}$$

$$\sum_{l=0}^{L-1} g_l g_{l+2n} \equiv \sum_{l=-\infty}^{\infty} g_l g_{l+2n} = 0 \tag{14}$$

Additional to the above conditions, Daubechies (1988) specified vanishing moment conditions on the wavelet function and led to obtain the scaling filters which have minimum delay. In this study Daubechies filter of width 8 is used for the DWT. Actual value and the shape are expressed on Figure 1 and Table 1.

Table 1 Daubechies wavelet and scaling filters of width 8.

l	Wavelet filter (h_l)	Scaling filter (g_l)
0	-0.010597401785	0.230377813309
1	-0.032883011667	0.714846570553
2	0.030841381836	0.630880767930
3	0.187034811719	-0.027983769417
4	-0.027983769417	-0.187034811719
5	-0.630880767930	0.030841381836
6	0.714846570553	0.032883011667
7	-0.230377813309	-0.010597401785

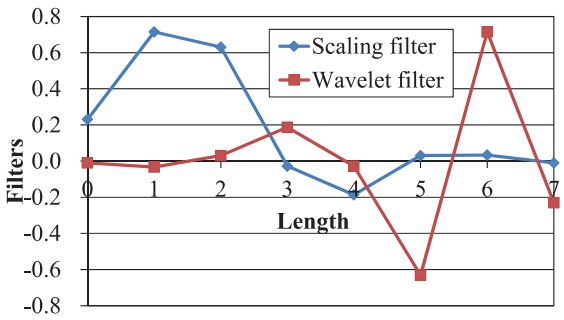

Figure 1 Daubechies wavelet and scaling filters of width 8.

3. DISCRETE WAVELET PACKET TRANSFORM

As shown in the previous section, the DWT decomposes the frequency interval $0 \le f \le 1/2\Delta t$ into adjacent individual intervals. The DWPT can be regarded as one of the extension of orthonormal transformation and decomposes the frequency into 2^j equal and individual intervals at the level j. The actual procedure of the calculation is readily

expressed using very simple modification of the pyramid algorithm (Percival and Walden 2000).

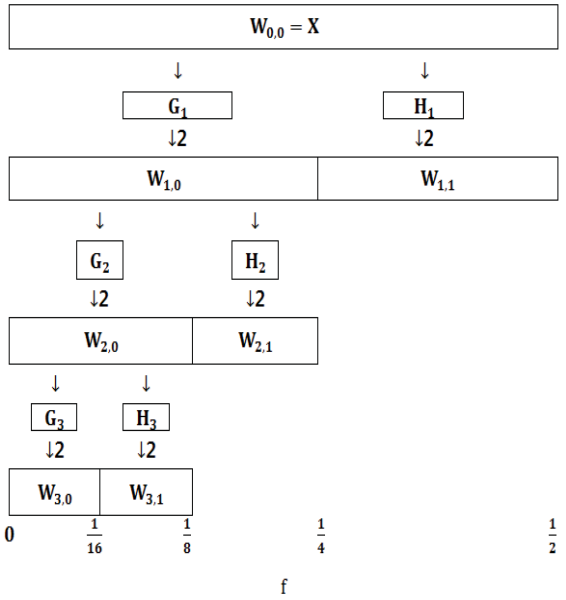

Figure 2 Flow diagram illustrating the analysis of $\mathbf{X}$ into $\mathbf{W}_{3,0}$, $\mathbf{W}_{3,1}$, $\mathbf{W}_{2,1}$ and $\mathbf{W}_{1,1}$ which is identical to partial DWT of level 3.

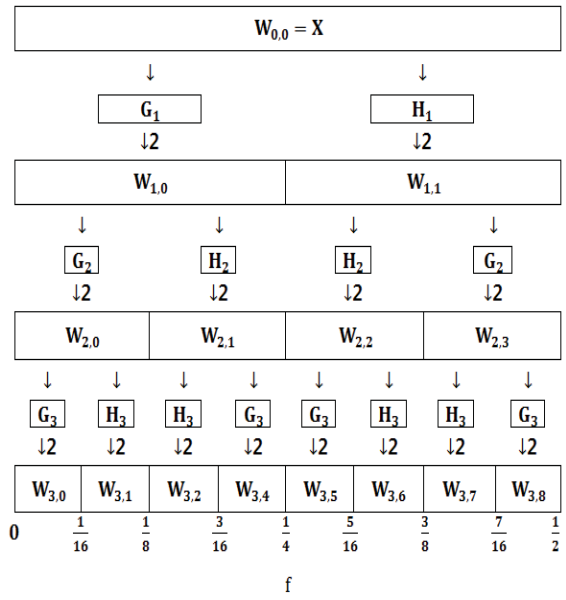

Figure 3 Flow diagram illustrating the analysis of $\mathbf{X}$ into $\mathbf{W}_{3,0}$, $\mathbf{W}_{3,1}$, …, $\mathbf{W}_{3,8}$ using DWPT of level 3.

Figure 2 shows the flow diagram of the DWT pyramid algorithm described in the previous section, where the level J_0=3. The starting point is defined as $\mathbf{W}_{0,0} = \mathbf{V}_0 = \mathbf{X}$ and other nodes represent $\mathbf{W}_{1,1} = \mathbf{W}_1$, $\mathbf{W}_{2,1} = \mathbf{W}_2$, $\mathbf{W}_{3,1} = \mathbf{W}_3$ and $\mathbf{W}_{3,0} = \mathbf{V}_3$. G_j and H_j represent filtering with use of the wavelet filter $\{h_l\}$ and the scaling filter $\{g_l\}$ at the level j. The '$\downarrow 2$' denotes the "down-sampling by two". The fractions at the lowest level denote the corresponding frequencies with Δt=1.

By using the low-pass and high-pass filters, the process of the decomposition of time series $\mathbf{X}$ is simply illustrated in the figure. It should be noted, however, that the nominal frequency intervals for these four nodes are not constant.

Figure 3 shows the flow diagram of the DWPT. It can be seen that the frequency intervals are constant and the resolution is improved by the iterative use of the low-pass and high-pass filters. This is the reason for the introduction of the DWPT.

4. FULL SCALE EXPERIMENT

The full scale ship experiment was carried out on January 25th 2012 using the training ship Shioji-maru of Tokyo University of Marine Science and Technology. A photo and principal particulars of the ship are shown in Figure 4 and Table 2. The location of the experimental area was off Sunosaki cape in Chiba Prefecture, Japan.

Figure 4 The training ship Shioji-maru.

Table 2 Principal particulars of the ship.

Length (P.P.)	46.00(m)
Breadth (M_{LD})	10.00(m)

Depth (M_{LD})	6.10(m)
Draught (M_{LD})	2.65(m)
Displacement	659.4(t)

Figure 5 shows the trajectory of the T.S. Shioji-maru during the experiment. The blue arrow denotes the main direction of waves. In order to measure changes in ship motions with respect to the encounter angle of waves, the angle of CPP was set to 10.5 degrees during 90 minute manoeuvres involving straight sections and changes in course.

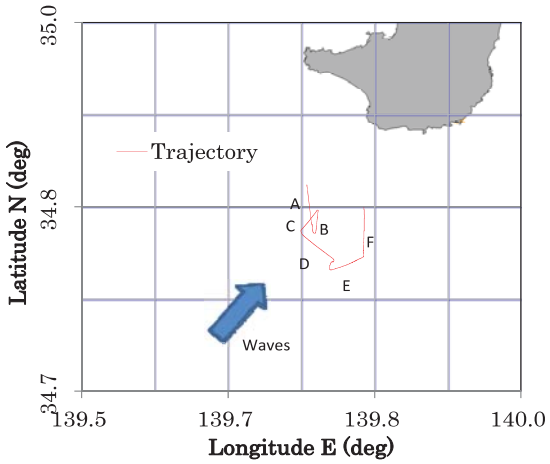

Figure 5 The experimental area at the south of Sunosaki cape and the ship trajectory.

Table 3 Ship course and the sea conditions.

Run	Ship course (deg)	Ship speed (knot)	Wind direction (deg)	Wind speed (m/s)
A	180	8.3	257	10.4
B	0	10.4	260	11.5
C	240	7.3	265	11.5
D	120	9.9	258	11.8
E	60	10.7	267	11.5
F	0	10.5	267	11.4

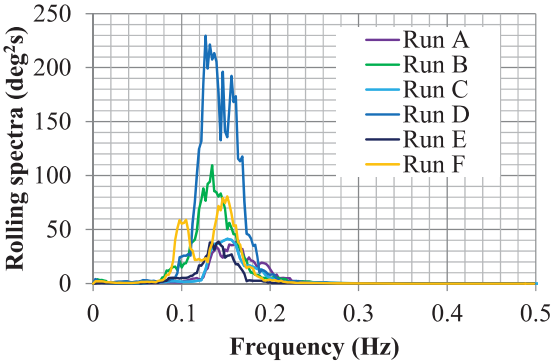

Figure 6 Power spectra of rolling motions.

Table 3 shows the courses and the mean speed-through-water of the ship, and true wind directions and the speeds are also summarized. During the experiment, observed wind waves were: height 1.0-1.5m, period 6-7 sec, direction 200-240 degrees, and swells were: height 2-3m, period 8-10 sec, direction 200 degrees. Note that the wave conditions listed in Table 3 can be recognized rather severe, since the ship is not a large ship (Table 2).

Figure 6 shows power spectra of the rolling motion calculated by FFT. It should be noted that the spectra "D" and "E" show the large difference in spite of adjacent run, because there is a large course alteration between them.

In this paper, the rolling time series between "D" and "E" are analysed in order to concentrate our attention on the non-stationarity. The trajectory is indicated in Figure 7 and seems to be a zigzag line because of beam seas. The analysed time span is 102.4s.

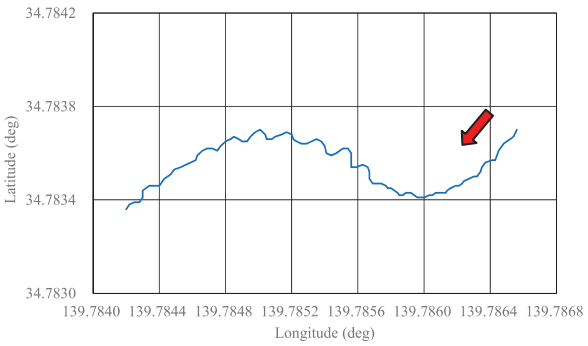

Figure 7 Time series of rolling motion. The red arrow denotes the starting side.

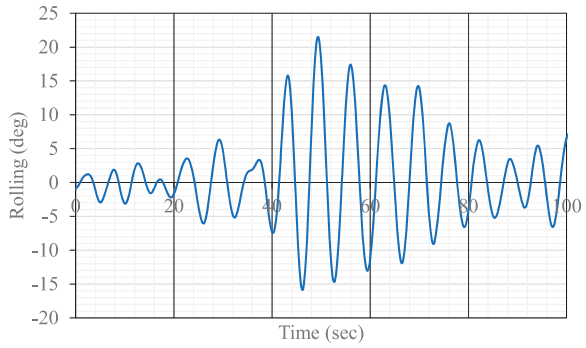

Figure 8 Time series of rolling motion.

Figure 8 shows the time history of the rolling motion that was analysed. The sampling time is 0.1s and 1024 observations are included. It can be seen that the ship was experienced rather large amplitude rolling during the beam seas condition (40 to 70 sec).

Figure 9 shows the power spectrum analysed by DFT ignoring the fact that the data is non-stationary. The peak frequency is 0.152Hz and coincides with the rolling natural frequency of the ship.

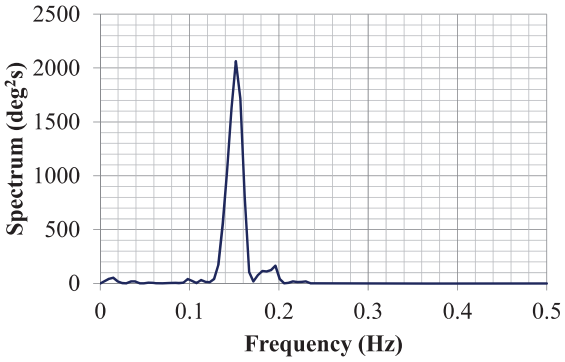

Figure 9 Power spectrum of rolling motion.

5. TVVAR MODEL ANALYSIS

TVVAR modelling was originally applied to analysis of the earthquake data (Kitagawa & Gersch, 1985, Jiang & Kitagawa, 1993). Generally, TVVAR models are transformed into state-space models, and the time varying coefficients can be evaluated by using the Kalman filter algorithm. Using the estimated time varying coefficients, the instantaneous power spectra of ship motions can be estimated at every moment.

Figure 10 shows the time evolution of the estimated auto spectra of roll angle from 0s to 100s. In this figure, the curves denote estimated instantaneous auto spectra and are superimposed on time axis with time increasing. In this estimation, the model order was set to 9. Comparing with the ship trajectory illustrated in Figure 8, it is found that the rolling motion becomes larger during the beam seas and the peak frequency coincides well with figure 9. On the other hand, it can be seen the "development period" at the beginning of analysis (from 0s to 30s). This comes from the initial conditions of the Kalman filter and means that the TVVAR modelling analysis requires a certain length of time series. In addition to this, some problems were pointed out in the TVVAR modelling. The maximum likelihood method for determination of the trade-off parameter, which is the ratio of the observation noise and the system noise of Kalman filter, cannot be applied to the real-time algorithm.

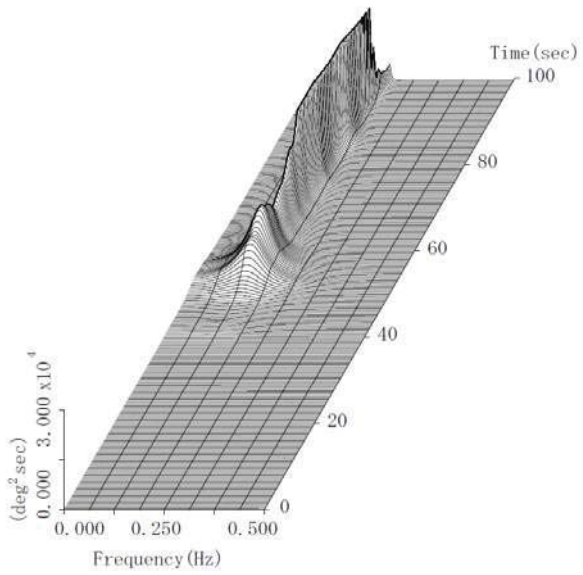

Figure 10 Instantaneous auto spectrum of rolling motions estimated by TVVAR modelling.

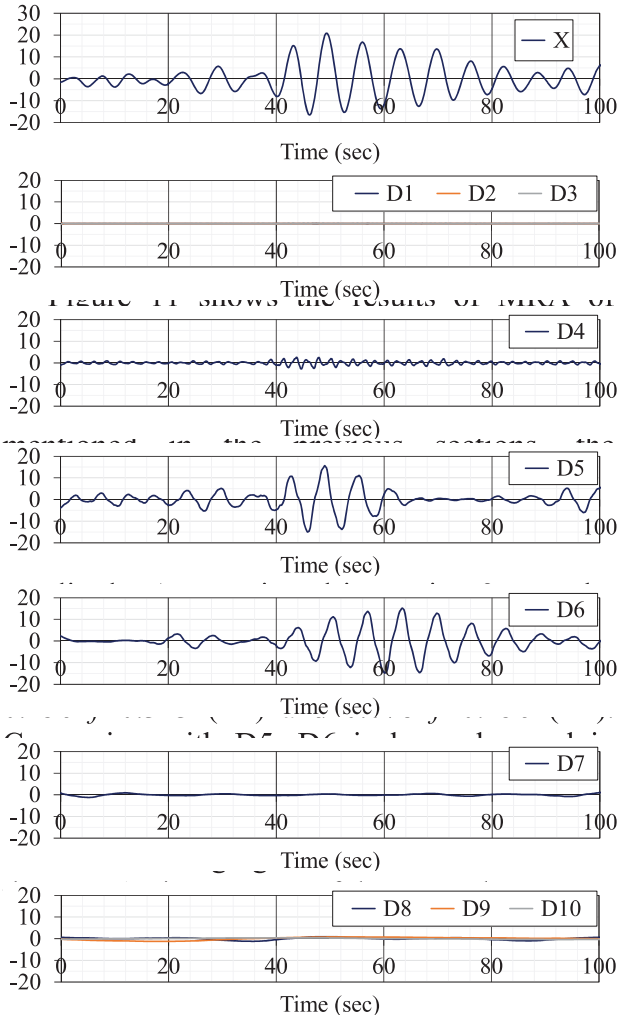

Figure 11 Results of multi-resolution analysis of rolling motion time series.

Figure 12 shows the time evolution of the estimated DWT spectrum from 0s to 100s. The DWT spectrum is expressed by discrete value, therefore, the graph is indicated in a stepwise shape. In this figure, levels of the DWT can be seen from 4 to 10 because frequencies of the smaller level are higher than 0.5Hz. The wide band on the centre (around 0.25Hz) denotes the power of D5 and the neighbouring left band denotes the power of D6. Similar to Figure 11, it can be observed that D6 is less advanced in development and has long duration, comparing with D5. This conclude that the DWT analysis is very useful for frequency/time analysis.

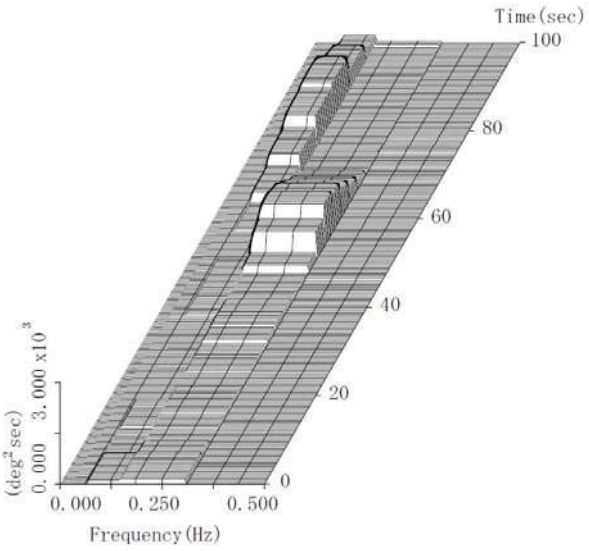

Figure 12 Results of DWT analysis of rolling motion.

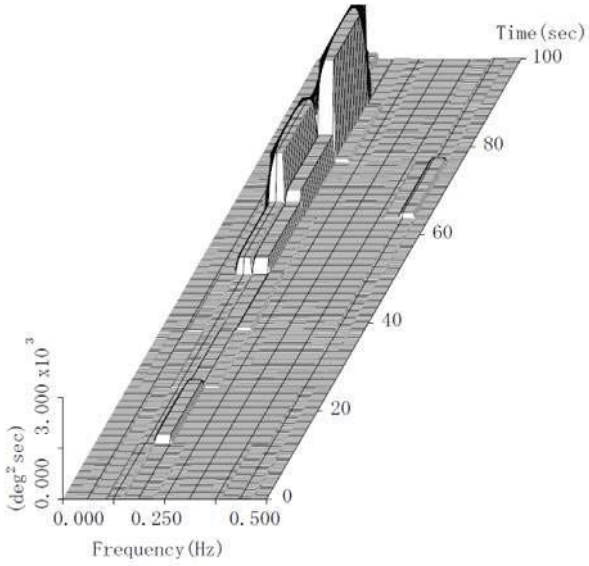

Figure 13 Results of DWPT analysis of level 7 of rolling motion.

Figure 13 shows the time evolution of the estimated DWPT spectrum of level 7. As described in the section 3, the frequency intervals are unified and the resolution is improved than DWT analysis. The peaks of the spectra were sharpened in the frequency-wise. Furthermore, the shape of spectra agree well

with the results of DFT and TVVAR modelling. However, it can be also seen that the resolution in time is worsened in comparison with Figure 12. Therefore, selection of the suitable level is very important for the effective DWPT analysis.

7. CONCULSIONS

The DWT and DWPT were applied to non-stationary ship motion data. Comparing to the spectra of DFT and the TVVAR modelling, the results obtained in this report can be summarized below:

(1) The MRA can be applied to analyses of non-stationary time series. It is very useful to extract the motion that has a certain frequency band.

(2) The locations of peaks of DWT spectra represent the time evolution of the rolling motion and agree well with the peaks of the spectra estimated by TVVAR modelling.

(3) Selecting a suitable level, the spectra estimated by the DWPT analysis agree well with the results of DFT and TVVAR modelling.

This concludes that the DWT and DWPT are powerful tools for analysing non-stationary ship motion data.

8. ACKNOWLEDMENTS

This work is partly supported by Grant-in-Aid for Scientific Research of the Japan Society for Promotion of Science (No. 26420822). The author expresses sincere gratitude to the above organizations and thanks the captain and crew of the training ship Shioji-maru.

9. REFERENCES

Daubechies, I., 1988, "Orthonormal Bases of Compactly Supported Wavelets", Communications on Pure and Applied Mathematics, 41, pp.909-996.

Iseki, T., Terada, D, 2002, "Study on Real-time Estimation of the Ship Motion Cross Spectra," Journal of Marine Science and Technology, Vol.7, pp.157-163.

Iseki, T., 2006, "Instantaneous Spectral Analysis of Non-stationary Ship Motion Data", Proceedings of the 25th International Conference on Offshore Mechanics and Arctic Engineering, OMAE2006-92197.

Jiang, X. Q., Kitagawa, G., 1993, "A Time Varying Coefficient Vector AR Modeling of Non-stationary Covariance Time Series," Signal Processing, 33, No.3, p.315-331.

Kang, B. and Iseki, T., 2013, "Application of Discrete Wavelet Transform to Ship Motion Analysis", Proceedings of Asia Navigation Conference 2013(ANC2013), pp.20-26.

Kitagawa, G., Gersch, W., 1985, "A Smoothness Priors Time-Varying AR Coefficient Modeling of Nonstationary Covariance Time Series," IEEE Trans. Automatic Control, AC-30, No.1, January, pp.48-56.

Mallat, S.G., 1989, "A Theory for Multiresolution Signal Decomposition", The Wavelet Representation, IEEE Trans. Pattern Analysis and Machine Intelligence, 11, p.674-93.

Percival, D.B. and Walden, A.T., 2000, "Wavelet Methods for Time Series Analysis", Cambridge Series in Statistical and Probabilistic Mathematics, Cambridge University press.